Hindawi
Advances in Condensed Matter Physics
Volume 2023, Article ID 2902298, 6 pages
https://doi.org/10.1155/2023/2902298

Research Article

Computation of the Dielectric and Optical Properties of Dimethylammonium Tin Triiodostanate (II) Perovskite for Solar Cell Application

Perpetua Jelimo Chemaoi, Philip Otieno Nyawere, and Christopher Mkirema Maghanga

Kabarak University, P.O. Box 20157, Kabarak, Kenya

Correspondence should be addressed to Perpetua Jelimo Chemaoi; pchemaoi@kabarak.ac.ke

Received 16 June 2023; Revised 30 July 2023; Accepted 25 August 2023; Published 28 September 2023

Academic Editor: Upendra Kumar

Hybrid halide perovskites are promising photovoltaic materials for use in solar cells. The ongoing research on perovskites have shown that these materials are potential light-harvesting mediums. The optical properties of dimethylammonium triiodostanate (II) (DASnI3) a hybrid halide perovskites needs to be studied because it can be a good light absorber material due to the wide band gap exhibited. The real and the imaginary parts of the dielectric is a measure of the extent of light absorption. The GGA+U exchange-correlation implemented in Quantum ESPRESSO was used basing on density functional theory to obtain the optical properties. The DASnI3 has a direct band gap of 2.7 eV with the real part of the dielectric diagram indicating that the maximum value of ε_1 (ω) is in the visible range of (3.0–3.5 eV). High absorption peaks were also observed in the visible spectral region at energy of around (3.5–4.5 eV) with several weak peaks observed in the energy range of (4.5–14.0 eV). The band structure and the dielectric functions are important in the study of optical properties. These properties expresses the interaction of light with the material medium and thus the luminescence of the device which are important in the use of DASnI3 as a solar cell material in photovoltaics.

1. Introduction

Optics is a study of properties that involves the interaction of light wave and a medium. Optical properties of materials are obtained by studying the polarization as well as the absorption of light within electromagnetic radiation range in the medium. The luminescence of a device depends on the properties of a medium as they are observed when the ion and the host interact [1]. Lead halide-based solar cells such as FAPbI3 perovskite show a power conversion efficiency of 25.2% [2]. These efficiencies are high hence the solar cell is approaching a stage for commercialization due to their unique luminescence properties [3]. These materials are said to be exhibiting very high photoluminescence (PL) quantum efficiencies when at room temperature. These lead halide perovskites properties are also made under simple and inexpensive fabrication method [4]. Photon recycling for both free-carrier and exciton luminescence has been observed from various materials because of their high PL quantum efficiencies. High PL quantum efficiency enables the perovskites new optical functionality as light-emitting devices [5]. However, it has been proven that lead is toxic and thus poses a health risk when it leaches to the environment. Therefore, there is a need to study other perovskites like the dimethylammonium triiodostanate (II) (DASnI3) with similar properties as lead halide perovskites as alternative materials.

To analyze the optical properties of materials it is necessary to study the band gap energy of a semiconductor to be considered in its application as a solar cell material. A direct band gap material is considered to be more efficient as compared to an indirect band gap material to be used as an optoelectronic material due to phonon involvement which makes an indirect band gap semiconductors a poor emitter [6]. Through the detailed balance principle, the band gap is used in determining the theoretical upper limit of a cell's efficiency. From the principle, the band gap (Eg) depends

greatly on the PL quantum efficiency of a material used. The recombination dynamics is key in determining the (PL) quantum efficiency of the photocarriers of the material. The synthesis and the optical characterization of CsSnX by Jellicoe et al. [7] on a nanocrystal perovskites, showed that the band gap can be tuned by the adjustment of the halide composition and also the spatial confinement. While the structure depended on deposition temperature [8]. From the results of Jellicoe et al. [7], it indicated that the species of nanocrystals they studied adopted the perovskites structures. They also performed transient PL on optical properties using solution dispersed particles, they observed some spectral shifts. This indicated that a good optical property can be obtained to be used for solar cell application.

2. Methodology

The study of DASnI3 by first principle computation of the properties was undertaken using density functional theory (DFT) [9]. This was done basing on plane waves which is a self-consistent field and norm conserving and done in the framework of Perdew et al. [10] using generalized gradient approximation (GGA+U). All the calculations were done using the simulation code Quantum ESPRESSO [11]. Optimization of the cell dimension obtaining of the k-points, and also the cutoff values for the kinetic energy were done and values which were accurate were obtained by graphing. Using proper basis sets the ground state convergence of energy which is at the minimum convergence threshold were obtained [12].

Optical properties of DASnI3 are expressed using the dielectric constant (ε_1) the conductivity ($\sigma_{1)}$, and the permeability (μ_1) in a matter. In studying the properties, it is required that the properties of the complex refractive index which is a new response function be defined in the form;

$$\widehat{N} = n + ik = \left[\varepsilon_1\mu_1 + i\frac{4\pi\varepsilon_1\sigma_1}{\omega}\right]^{\frac{1}{2}} = [\widehat{\varepsilon}\mu_1]^{\frac{1}{2}}. \tag{1}$$

To write an equation for the refractive index (n) of the material, it requires that we have the conductivity (σ_1), the permeability (μ_1), and also the dielectric constant (ε_1). These constants can also be used to write an equation for the extinction coefficient (k) as shown in Equation (2).

$$\widehat{n}^2 = \frac{\mu_1}{2}\left\{\left[\varepsilon_1^2 + \left(\frac{4\pi\sigma_1}{\omega}\right)^2\right]^{\frac{1}{2}} + \varepsilon_1\right\}, \tag{2}$$

$$\widehat{k}^2 = \frac{\mu_1}{2}\left\{\left[\varepsilon_1^2 + \left(\frac{4\pi\sigma_1}{\omega}\right)^2\right]^{\frac{1}{2}} - \varepsilon_1\right\}. \tag{3}$$

Equations (2) and (3) are vital because they relate to the dynamical behavior of the material and also the propagation of electromagnetic wave in a material. In the study of polarization and absorption of electromagnetic radiation, it requires an expression in terms of dielectric functions within the material medium [13]. This is mathematically represented by the relation below;

$$\varepsilon(\omega) = \varepsilon_1(\omega) + \varepsilon_2(\omega). \tag{4}$$

The reflectivity ρ means that the materials dielectric constant without losses be written in terms of refractive as well as the extinction coefficient k [14], which becomes;

$$\widehat{q} = \frac{\omega}{c}\widehat{N} = \frac{n\omega}{c} + i\frac{k\omega}{c}, \tag{5}$$

$$n^2 - k^2 = \varepsilon_1\mu_1, \tag{6}$$

$$2nk = \frac{4\pi_1\mu_1\sigma_1}{\omega}. \tag{7}$$

Writing these equations in terms of dielectric constant (ε_1), permeability (μ_1), and conductivity (σ_1) will give,

$$\widehat{N}^2 = \mu_1\left[\varepsilon_1 + i\frac{4\pi\sigma_1}{\omega}\right] = \mu_1\widehat{\varepsilon} \approx \frac{4\pi_i\mu_2\sigma_1}{\omega}. \tag{8}$$

It is noted that $|\varepsilon_1| \geq 1$ when,

$$\left|\widehat{N}\right| = (n^2 + k^2)^{\frac{1}{2}}. \tag{9}$$

2.1. Reflectivity. The reflectivity ρ (ω) can also be expressed mathematically as,

$$\rho(\omega) = \left[\frac{1 - \widehat{N}}{1 + \widehat{N}}\right]^2 = \frac{(1-n)^2 + k^2}{(1+n)^2 + k^2}. \tag{10}$$

From the equation above when K becomes 0 then Equation (10) reduces to Equation (11).

$$\rho = \left|\frac{1-n}{1+n}\right|^2. \tag{11}$$

Summing over conduction bands, we obtain the dielectric function ε_1 (ω) imaginary part by Equation (12).

$$\varepsilon_{\alpha\beta}^{(1)}(\omega) = \frac{4\pi^2e^2}{\Omega}\frac{1}{q^2}\lim_{q\to 0}\Sigma_{c,v,k}2\omega_k\delta(\in_{ck} - \in_{vk} - \omega) \times \left\langle u_{ck+eq}|u_{vk}\right\rangle. \tag{12}$$

Equation (12) is an indication of the transition of the occupied and those states which are unoccupied in the first level of the Brillion zone with fixed k wave vectors. The Kramers Kronig is a relation used to connect the real part and the imaginary part of a function which is given as;

$$\varepsilon_{\alpha\beta}^{(1)} = 1 + \frac{2}{\Pi} p \int_0^{\infty} \frac{\varepsilon_{\alpha\beta}^{(2)}(\omega')\omega'}{\omega^{2'} - \omega^2 i\eta} d\omega'. \quad (13)$$

Here, dielectric constant denoted by $(\widehat{\varepsilon})$ and the conductivity $(\widehat{\sigma})$ are said to be the main response functions on an electric field.

2.2. The Absorption Coefficiency. The absorption coefficiency $I(x) = I_o \exp(-ax)$ which is equivalent to the intensity loss for a given length is given as follows:

$$\alpha(\omega) = \frac{\omega}{4\pi} \varepsilon_2(\omega). \quad (14)$$

Equation (14) above shows the existence of a strong relationship between the absorption coefficient and the imaginary part of the dielectric [15]. Using Quantum ESPRESSO hybrid functionals the dielectric matrix which depends on the frequency was calculated where the imaginary and the real dielectric values of DASnI3 were obtained. The reflectivity and the refractive index were obtained by calculating the imaginary and the real part of the dielectric functions.

The refractive index of a material $\overline{n}$ is also obtained by calculation after evaluation of $\varepsilon_1(\omega)$ and $\varepsilon_2(\omega)$ as shown below.

$$\widetilde{n} = n(\omega) + ik(\omega)\sqrt{\varepsilon(\omega)}. \quad (15)$$

The refractive index is represented by the real refractive index given by a ratio between the phonon speed and the vacuum speed of a photo in a material.

3. Results and Discussion

It is observed that DASnI3 is a semiconductor exhibiting a 2.7 eV direct and a wide band gap at gamma symmetry points which is comparable to 2.98 eV for DA iodide bismuth a halide perovskite material [16]. This value obtained for DASnI3 is reasonable because it is well known that DFT usually underestimates a materials band gap. The band structure calculated for the orthorhombic phase DASnI3 crystal based on lines of high symmetry in the first Brillouin zone indicated a Fermi level which is in between the bands. There are characteristic peaks that could be attributed to the direct interband transition between the filled iodine 5p and the tin 5s valence band maximum (VBM) states to the empty conduction band minimum (CBM) tin and iodine 5p orbitals. The decrease in the overlap of the metal orbital and the halide orbital caused by the dimethylammonium which alters BX6 octahedral size. This affects the band gap by pushing the valence band away from the vacuum causing a large dispersion between the bands. A large band gap causes carrier effective masses to be small. A material with a wide gap is beneficial in healing deep trap defects and the results is a material that is tolerant to defects. Density of states (D.O.S) is frequently used when studying the materials properties which are physical which includes the dielectric, the photoemission spectra, as well as the transport properties. D.O.S shows the location and the role of different energy orbitals especially those involved in the formation of the band structure. The energy in the tin 5s which is high and occupies the VBM are responsible mainly for the good photovoltaic properties due to their stability with respect to decomposition.

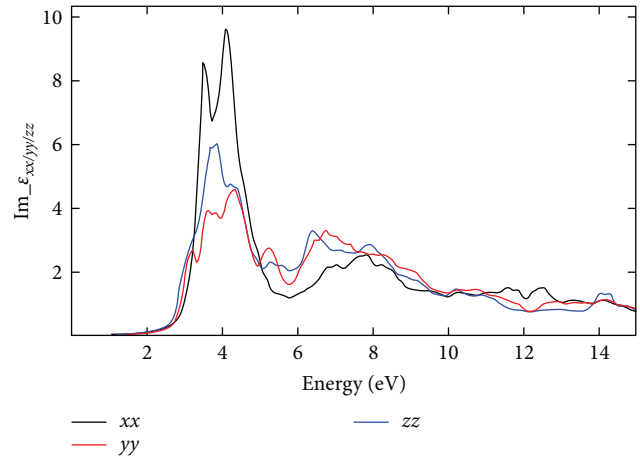

FIGURE 1: Imaginary part of the dielectric.

Optical properties of a material are described by its absorption coefficient $\alpha(\omega)$, extinction coefficient $k(\omega)$, reflectivity $\rho(\omega)$, and function of electron energy loss $L(\omega)$ calculated in photon energy terms dependent on dielectric function. The real part and the imaginary part of the dielectric can be used in calculating the properties [17]. Mathematical presentation of polarization and absorption of the electromagnetic radiation dielectric functions is given by the relation;

$$\varepsilon(\omega) = \varepsilon_1(\omega) + i\varepsilon_2(\omega). \quad (16)$$

Equation (16) above is the dielectric function equation where $\varepsilon_1(\omega)$ which is the first term, representing the real part, shows the light polarization, the imaginary part is represented by the second term $\varepsilon_2(\omega)$ of the dielectric function, which measures the extent of light absorption. The calculated static dielectric constant $\varepsilon_1(0)$ for DASnI3 is 4.0 which is comparable to MAPbI with static dielectric constant of 6.0 has a band gap of 1.7 eV [1] CsPbI3 has a static dielectric of 5.0 with a band gap energy of 1.73 eV [18] and EASnI3 with static energy of 5.38 has a band gap of 1.17 eV [19]. Comparing the values indicates that $\varepsilon_1(0)$ increases with the decrease in the band gap indicating that the band gap energy and $\varepsilon_1(0)$ are inversely proportional showing a consistency to Penn [20] model. The DASnI3 compound has a slightly lower value of $\varepsilon_1(0)$ compared with that of MAPbI3 and CsPbI3 while the MASnI3 has highest value due to the small band gap. Figure 1 below shows the graph of imaginary part plotted against energy in electron volts.

Figure 2 below is a graph of the real part of the dielectric drawn against the energy which measures the extent of light polarization.

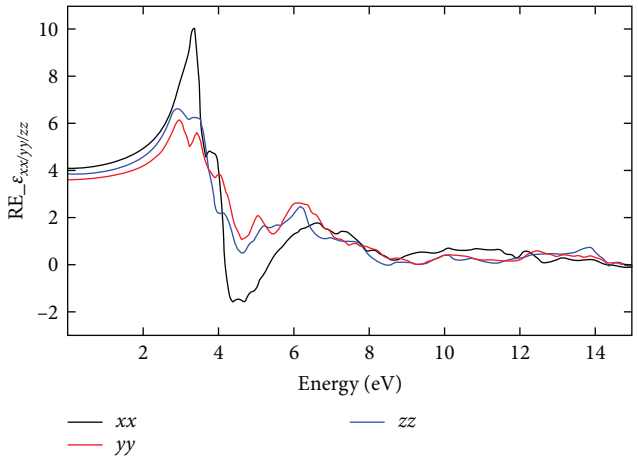

Figure 2: Graph of the real part against energy in electron volts of the dielectric.

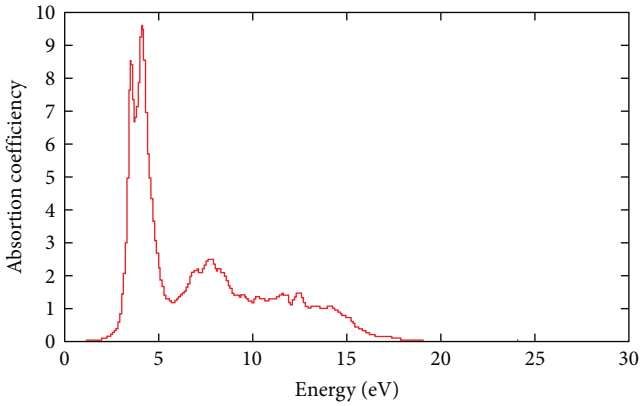

Figure 3: Absorption coefficient against energy in electron volts graph.

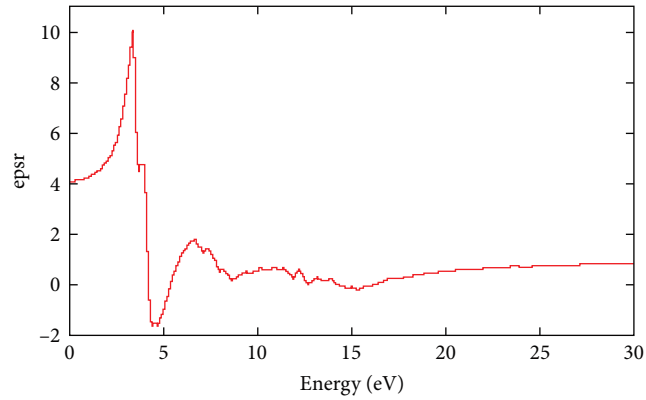

Figure 4: Graph of the real part of the complex refractive index against energy.

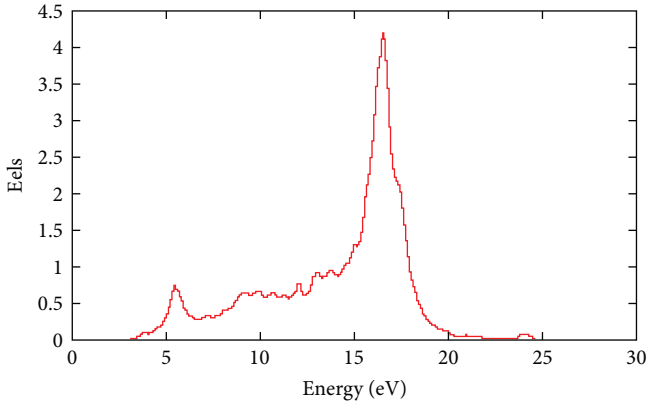

Figure 5: Electron energy loss against energy in electron volts.

It is shown that dimethylammonium tin iodide has a remarkably large value of ε_1 (0) = 4.0 which is comparable to that of MAPbI3 with a value of ε_1 (0) = 6.00 and that of CsPbI3 ε_1 (0) = 6.00. From Figure 2 above, the highest value of ε_1 (ω) is around 3.5 eV which is within the visible range of the energy region and followed by decreasing small humps caused by the interband transitions between VBM and the CBM bands. While, the extent in which light is absorbed is measured using the imaginary part of the dielectric function. High absorption peak of the range 3.5–4.5 eV is observed in the visible spectral region which is equivalent to 314–500 nm wavelength. This energy compares with the energy range of between 380 and 780 nm of the visible energy wavelength solar spectrum [21] translating to energy of around 1.6–3.5 eV. From our calculated results the maximum absorption wavelength of between 441 and 500 nm was obtained, weak peaks are also observed having an energy range between 4.5 and 14 eV. High absorption coefficient of DASnI3 indicates that this material absorbs photons readily having energy equal to the energy of the band gap energy. This energy excites electrons from the valence band to the conduction band. Figure 3 below shows the absorption coefficiency graph against energy.

Determination of fraction of absorbed incident energy in a material for a given length gives a materials absorption coefficient. The absorption coefficient α (ω) for DASnI3 increases beginning from zero as shown in Figure 3. The increase in energy is due to the higher energy of the phonon compared to band gap energy. The highest energy of the phonon is 4.8 eV which is a characteristic value to both insulators as well as semiconductors.

Figure 4 above shows the refractive index n (ω) against the energy of the photon. Refractive index is a key factor that determines if a material is suitable for optical applications. Comparing Figures 2 and 4, it is observed that n (ω) spectrum replicates the pattern in Figure 2 that is ε_1 (ω). The peak value for DASnI3 as shown in Figure 4 is around 3 eV which corresponds to yellow light basing on the electromagnetic spectrum energy range, which corresponds to the visible region.

The energy lost when the electrons are traveling fast is given by electron energy loss denoted L (ω). The value obtained for DASnI3 as shown in Figure 5 is high showing that DASnI3 has large transmission loss this could be due to the thin absorber thickness [22]. This is in agreement with Ahamad et al., who argued that large band gaps greater than 1.8 eV, results in light absorption loss [23]. This should be improved to obtain a better absorber material. Reflectivity

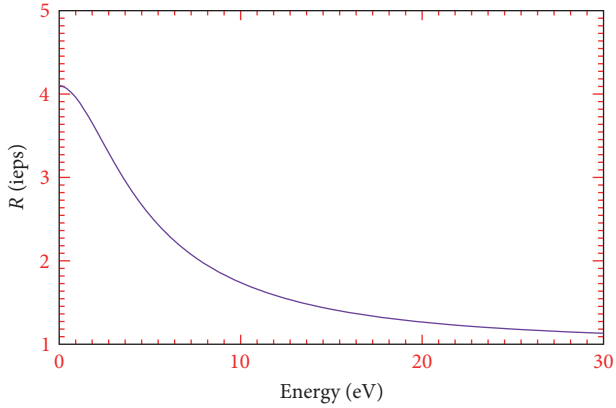

Figure 6: Reflexivity graph against energy in electron volts.

(ρ) represents the part of light reflected by a material from the incident energy. The highest value of reflectivity as shown in Figure 6 is 4.2 [24]. This is within the visible part of the electromagnetic spectrum indicating DASnI3 is a good material to absorb light.

4. Conclusions

We have reported on the optical properties of DASnI3 and from our reported results we found that they agree well with other studies both experimental and theoretical calculations. The calculation of the direct band gap compared with an indirect band gap material is more efficient, especially for optoelectronic applications due to phonons that makes a direct band gap semiconductor a good light emitter.

In the study of the imaginary part of the dielectric, two peaks were characteristic having the energy range between 2.5 and 4.5 eV equivalent to a wavelength of between 441 and 500 nm. This range is within the visible light region of the solar spectrum which indicates that DASnI3 having a band energy of 2.7 eV can absorb photons of energy equivalent to this energy. High absorption coefficient of DASnI3 indicates that the material readily absorbs photons with energy equal to the band gap energy. This energy is responsible for exciting electrons from the valence band to the conduction band.

The orthorhombic phase hexagonal structure of the dimethylammonium shows a high dielectric constant. This high value protects the active layer of the perovskite being positioned as the top layer hence a beneficial part of the perovskite. Therefore, in summary the lower temperature dimethylammonium indicating high absorption coefficient and dielectric functions is a potential material for application in solar materials fabrications. With experimental work, it should be verified that this material is appropriate for application. From this computational simulation, we conclude that this material is good for applications in fabrication for optical experimental solar cells.

Data Availability

Data supporting this research article are available from the corresponding author or first author on reasonable request.

Conflicts of Interest

The authors declare that they have no conflicts of interest.

Acknowledgments

This work has been done through the provision of high-computing facility of CHPC. We are indebted to them for the time resource provided that we have used to compute the optical properties of dimethylammonium triiodostanate II. Great appreciation goes to Kabarak University for the opportunity to do my (Perpetua Jelimo Chemaoi) MSc thesis. Much of this work was done while doing the thesis.

References

[1] Y.-L. Wang, S. Chang, X.-M. Chen et al., "Rapid growth of halide perovskite single crystals: from methods to optimization control," *Chinese Journal of Chemistry*, vol. 37, no. 6, pp. 616–629, 2019.

[2] M. Kim, J. Jeong, H. Lu et al., "Conformal quantum dot-SnO_2 layers as electron transporters for efficient perovskite solar cells," *Science*, vol. 375, no. 6578, pp. 302–306, 2022.

[3] Y. Kanemitsu and T. Handa, "Photophysics of metal halide perovskites: from materials to devices," *Japanese Journal of Applied Physics*, vol. 57, no. 9, Article ID 090101, 2018.

[4] T. Yamada, Y. Yamada, Y. Nakaike, A. Wakamiya, and Y. Kanemitsu, "Photon emission and reabsorption processes in $CH_3NH_3PbBr_3$ single crystals revealed by time-resolved two-photon-excitation photoluminescence microscopy," *Physical Review Applied*, vol. 7, no. 1, Article ID 014001, 2017.

[5] Y. Kanemitsu, T. Yamada, T. Handa, and M. Nagai, "Optical responses of lead halide perovskite semiconductors," *Semiconductor Science and Technology*, vol. 35, no. 9, Article ID 093001, 2020.

[6] M. Khan, J. Xu, N. Chen, and W. Cao, "First principle calculations of the electronic and optical properties of pure and (Mo, N) co-doped anatase TiO_2," *Journal of Alloys and Compounds*, vol. 513, pp. 539–545, 2012.

[7] T. C. Jellicoe, J. M. Richter, H. F. Glass et al., "Synthesis and optical properties of lead-free cesium tin halide perovskite nanocrystals," *Journal of the American Chemical Society*, vol. 138, no. 9, pp. 2941–2944, 2016.

[8] M. C. Maghanga, "Influence of deposition parameters on optical properties of sputtered tungsten oxide films," *International Journal of Thin Film Science and Technology*, vol. 7, no. 2, pp. 61–65, 2018.

[9] P. Hohenberg and W. Kohn, "Inhomogeneous electron gas," "*Physical Review*, vol. 136, no. 3B, pp. B864–B871, 1964.

[10] J. P. Perdew, K. Burke, and M. Ernzerhof, "Generalized gradient approximation made simple," *Physical Review Letters*, vol. 77, no. 18, pp. 3865–3868, 1996.

[11] P. Giannozzi, S. Baroni, N. Bonini et al., "Quantum ESPRESSO: a modular and open-source software project for quantum simulations of materials," *Journal of Physics: Condensed Matter*, vol. 21, no. 39, Article ID 395502, 2009.

[12] W. Kohn and L. J. Sham, "Self-consistent equations including exchange and correlation effects," *Physical Review*, vol. 140, no. 4A, pp. A1133–A1138, 1965.

[13] B. Quan, X. Liang, G. Ji et al., "Dielectric polarization in electromagnetic wave absorption: review and perspective," *Journal of Alloys and Compounds*, vol. 728, pp. 1065–1075, 2017.

[14] J. Simmons and K. S. Potter, *Optical Materials*, Academic Press, 2000.
[15] K. C. Bhamu, A. Soni, and J. Sahariya, "Revealing optoelectronic and transport properties of potential perovskites Cs_2PdX_6 (X = Cl, Br): a probe from density functional theory (DFT)," *Solar Energy*, vol. 162, pp. 336–343, 2018.
[16] H. Zhao, K. Chordiya, P. Leukkunen et al., "Dimethylammonium iodide stabilized bismuth halide perovskite photocatalyst for hydrogen evolution," *Nano Research*, vol. 14, no. 4, pp. 1116–1125, 2007.
[17] S. K. Tripathy and V. Kumar, "Electronic, elastic and optical properties of $ZnGeP_2$ semiconductor under hydrostatic pressures," *Materials Science and Engineering B*, vol. 182, pp. 52–58, 2014.
[18] M. Ahmad, G. Rehan, L. Ali et al., "Structural, electronic and optical properties of $CsPbX_3$ (X = Cl, Br, I) for energy storage and hybrid solar cell applications," *Journal of Alloys and Compounds*, vol. 705, pp. 828–839.
[19] T. K. Joshi, G. Sharma, and A. S. Verma, "Investigation of structural, electronic, optical and thermoelectric properties of ethylammonium tin iodide ($CH_3CH_2NH_3SnI_3$): an appropriate hybrid material for photovoltaic application," *Materials Science in Semiconductor Processing*, vol. 115, Article ID 105111, 2020.
[20] D. R. Penn, "Wave-number-dependent dielectric function of semiconductors," *Physical Review*, vol. 128, no. 5, Article ID 2093, 1962.
[21] L. Aarts, B. M. Van der Ende, and A. Meijerink, "Down conversion for solar cells in $NaYF_4$: Er, Yb," *Journal of Applied Physics*, vol. 106, no. 2, Article ID 023522, 2009.
[22] C. Bulutay, "Interband, intraband, and excited-state direct photon absorption of silicon and germanium nanocrystals embedded in a wide band-gap lattice," *Physical Review B*, vol. 76, no. 20, Article ID 205321, 2007.
[23] T. Handa, A. Wakamiya, and Y. Kanemitsu, "Photophysics of lead-free tin halide perovskite films and solar cells," *APL Materials*, vol. 7, no. 8, Article ID 080903, 2019.
[24] P. J. Chemaoi, "Computation of the properties of organic-inorganic tin halide perovskite for photovoltaic application; first principles approach," 2022.